

Supporting Information

**Steered Polymorphic Nanodomains in TiO<sub>2</sub> to Boost Visible-Light Photocatalytic Oxidation**

Zeju Zhang<sup>1 †</sup>, Mang Niu<sup>1 †</sup>, Wei Li<sup>1</sup>, Chenfeng Ding<sup>2, 5\*</sup>, Peitao Xie<sup>1</sup>, Yongxin Li<sup>1</sup>, Lili Chen<sup>1</sup>, Xiaopeng Lan<sup>1</sup>, Chunlei Liu<sup>1</sup>, Xiaodong Yan<sup>3</sup>, Xuewei Fu<sup>4</sup>, Yaochun Liu<sup>5</sup>, Yuan Liu<sup>1, 5\*</sup>, Dapeng Cao<sup>6</sup>, Jingjie Dai<sup>7</sup>, Xiaofen Hong<sup>8</sup>, Chunzhao Liu<sup>1\*</sup>

<sup>1</sup> State Key Laboratory of Bio-fibers and Eco-textiles, Institute of Biochemical Engineering, The Affiliated Qingdao Central Hospital of Qingdao University, College of Materials Science and Engineering, Qingdao University, Qingdao 266071, China

<sup>2</sup> Energy Materials and Surface Sciences Unit (EMSSU), Okinawa Institute of Science and Technology Graduate University (OIST), 1919-1 Tancha Kunigami-gun, Onna-son, Okinawa 904-0495, Japan

<sup>3</sup> Key Laboratory of Synthetic and Biological Colloids, Ministry of Education, School of Chemical and Material Engineering, Jiangnan University, Wuxi 214122, China

<sup>4</sup> College of Polymer Science and Engineering, State Key Laboratory of Polymer Materials Engineering, Sichuan University, Chengdu 610065, Sichuan, China

<sup>5</sup> Foshan (Southern China) Institute for New Materials, Foshan 528200, China

<sup>6</sup> Beijing Advanced Innovation Center for Soft Matter Science and Engineering, Beijing University of Chemical Technology, Beijing 100029, China.

<sup>7</sup> School of Mechanical and Electronic Engineering, Qingdao Binhai University, Qingdao 266555, Shandong, China.

<sup>8</sup> Zhejiang Rich Environmental Protection Technology Co., Ltd., Hangzhou 310000, China.

<sup>†</sup> These authors contributed equally.

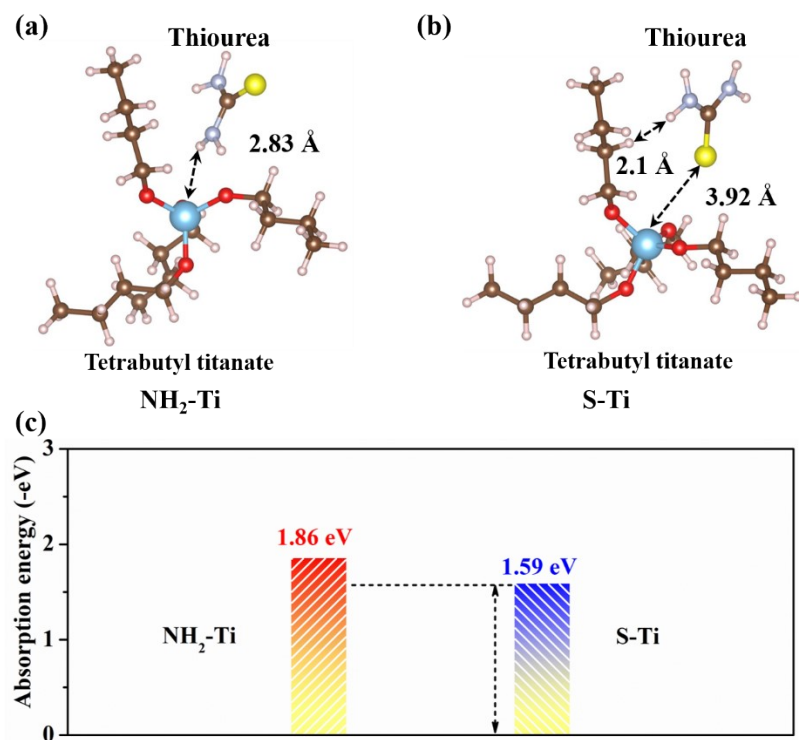


**Figure S1.** The simulated absorption structure of (a)  $\text{NH}_2$ -Ti and (b) S-Ti sites. (c) The comparison of absorption energy between  $\text{NH}_2$ -Ti and S-Ti sites.

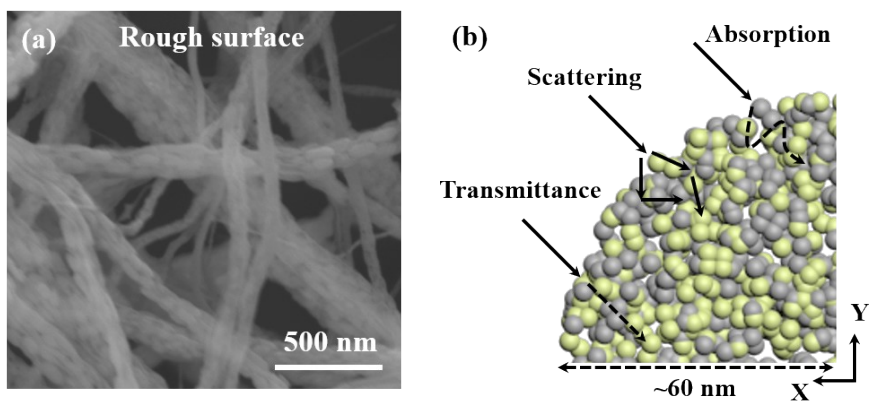


**Figure S2.** (a) SEM image of  $C_3N_4$ -induced  $TiO_2$  nanofibers. (b) Schematic mechanism of enhanced light harvesting of  $C_3N_4$ -induced  $TiO_2$  nanofibers.

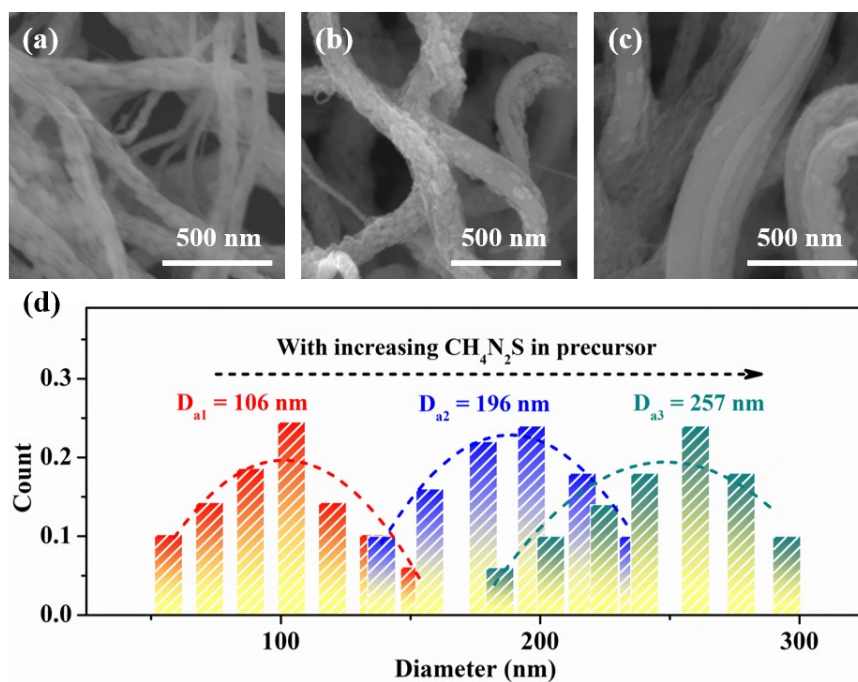


**Figure S3.** (a)-(c) SEM images of  $\text{C}_3\text{N}_4$ -induced  $\text{TiO}_2$  nanofibers with introduction various amount of thiourea into precursor. (d) Diameter distribution of nanofibers with increasing thiourea in precursor.

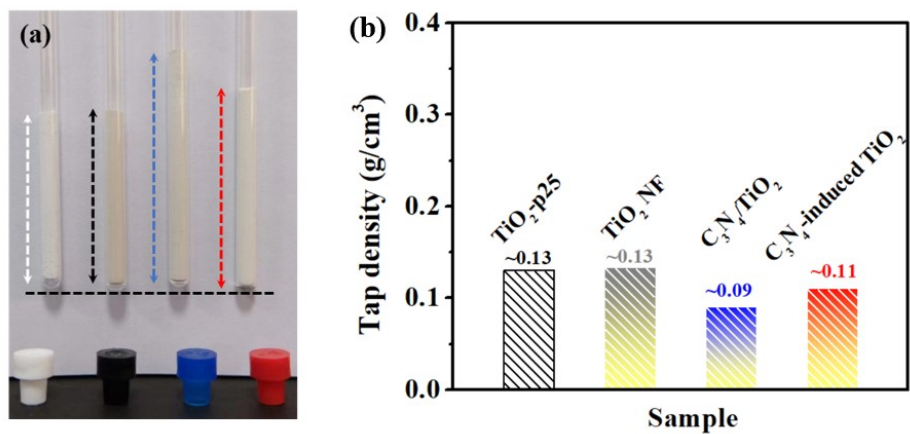


**Figure S4.** (a) Optical image and (b) tap densities of  $\text{TiO}_2\text{-P25}$ ,  $\text{TiO}_2\text{ NF}$ ,  $\text{C}_3\text{N}_4/\text{TiO}_2$ ,  $\text{C}_3\text{N}_4\text{-induced TiO}_2$ .

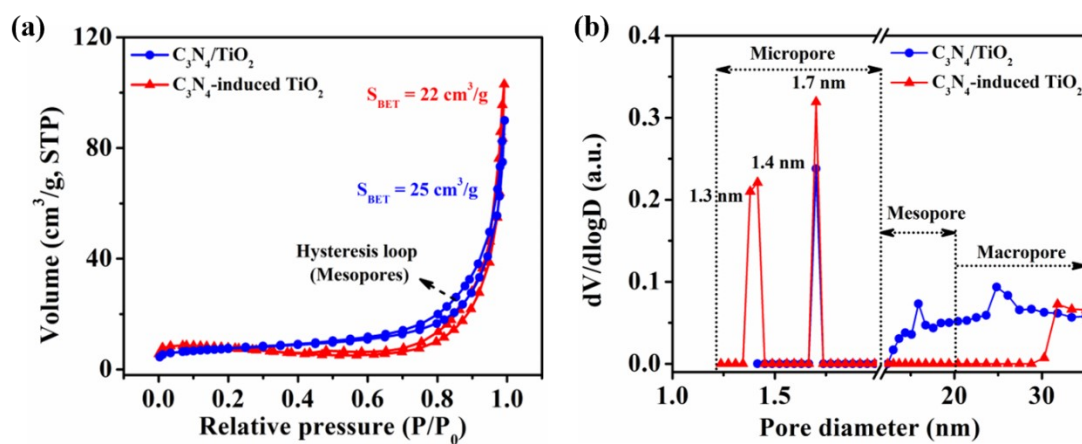


**Figure S5.** (a) Nitrogen adsorption/desorption curves and (b) pore size distribution of C<sub>3</sub>N<sub>4</sub>/TiO<sub>2</sub> and C<sub>3</sub>N<sub>4</sub>-induced TiO<sub>2</sub>.

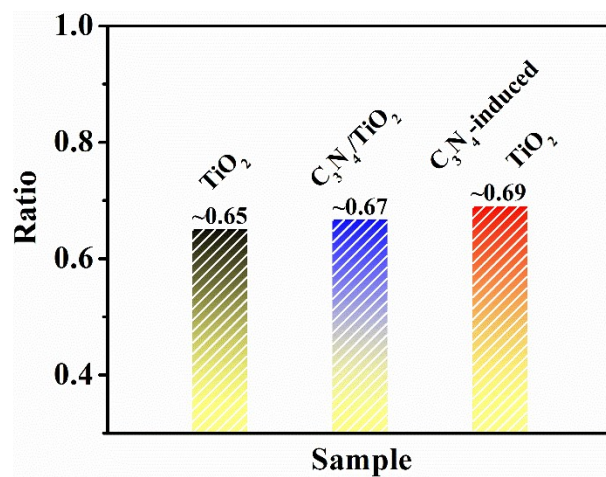


**Figure S6.** The relative intensity ratio of TiO<sub>2</sub> (004) peak to TiO<sub>2</sub> (200) peak according to the XRD patterns.

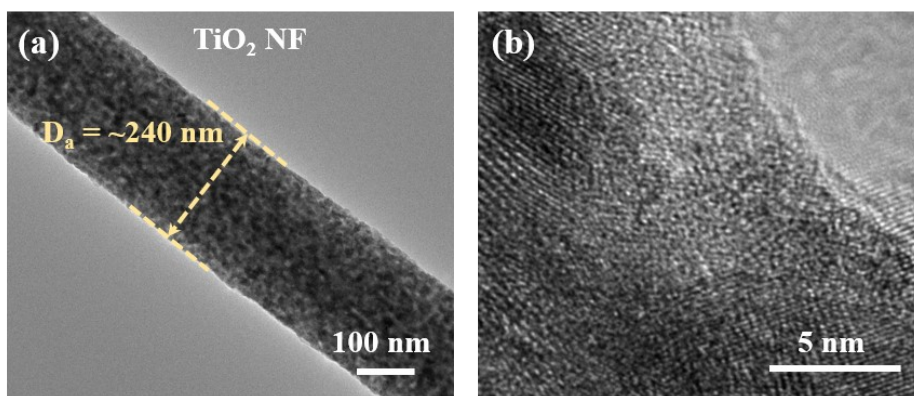


**Figure S7.** (a) TEM image and (b) HR-TEM image of TiO<sub>2</sub> nanofiber.



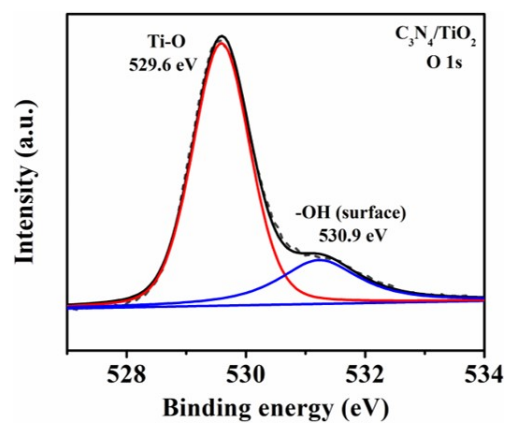


**Figure S8.** Gaussian fitted XPS curves of oxygen atoms in C<sub>3</sub>N<sub>4</sub>/TiO<sub>2</sub>.

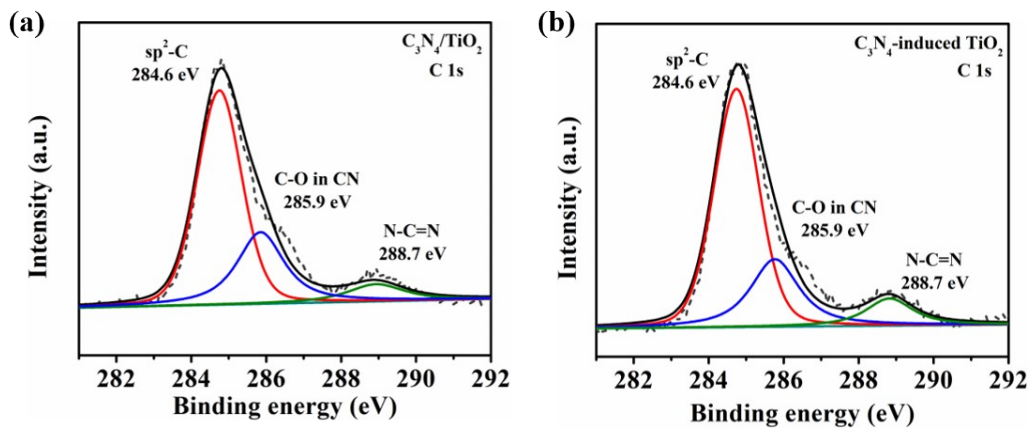


**Figure S9.** Gaussian fitted XPS curves of carbon atoms in (a)  $C_3N_4/TiO_2$  and (b)  $C_3N_4$ -induced  $TiO_2$ .

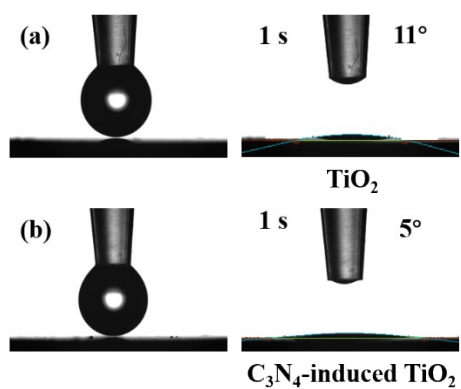


**Figure S10.** Contacting angle of water on the surface of (a)  $\text{TiO}_2$  and (b)  $\text{C}_3\text{N}_4$ -induced  $\text{TiO}_2$ .

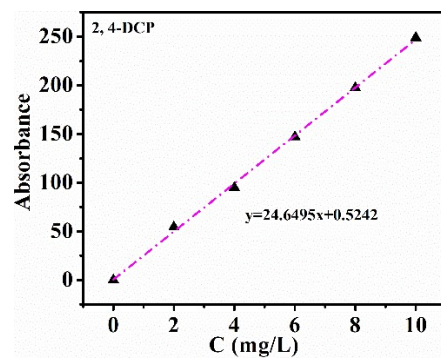


**Figure S11.** Standard curve of absorbance as a function of 2, 4-DCP concentration.

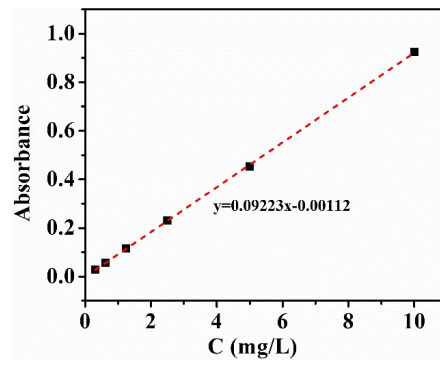


**Figure S12.** Standard curve of absorbance as a function of Rh-b concentration.

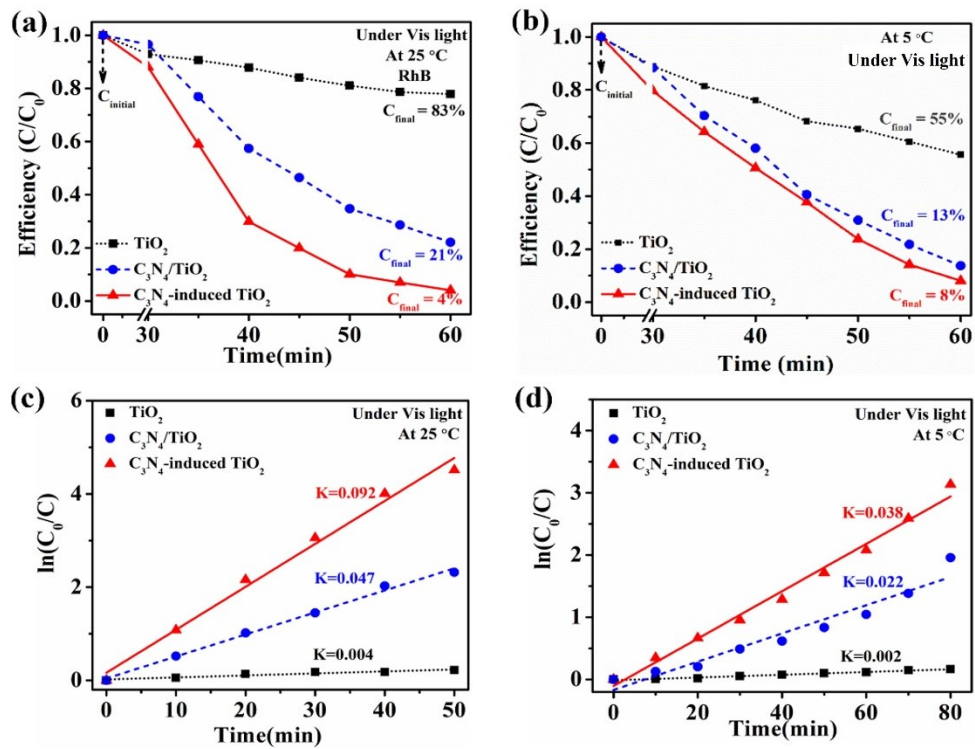


**Figure S13.** Photocatalytic degradation curves at (a) 25 and (b) 5 °C, and kinetic curves at (c) 25 and (d) 5 °C of TiO<sub>2</sub>, C<sub>3</sub>N<sub>4</sub>/TiO<sub>2</sub> and C<sub>3</sub>N<sub>4</sub>-induced TiO<sub>2</sub> on Rh-b.

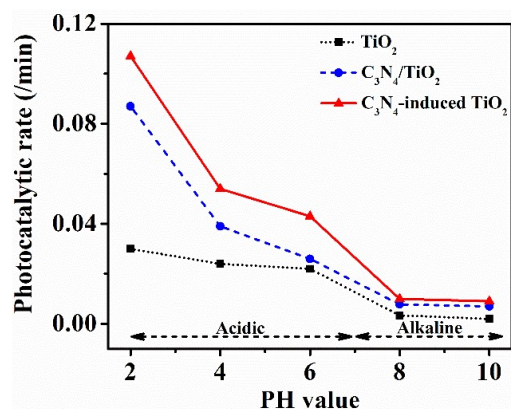


**Figure S14.** Photocatalytic degradation rate of  $\text{TiO}_2$ ,  $\text{C}_3\text{N}_4/\text{TiO}_2$  and  $\text{C}_3\text{N}_4$ -induced  $\text{TiO}_2$  under different PH values.

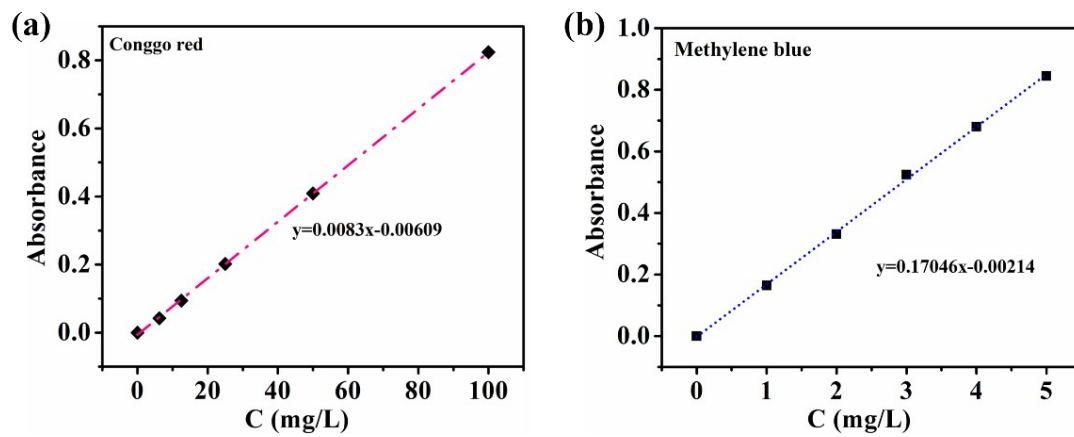
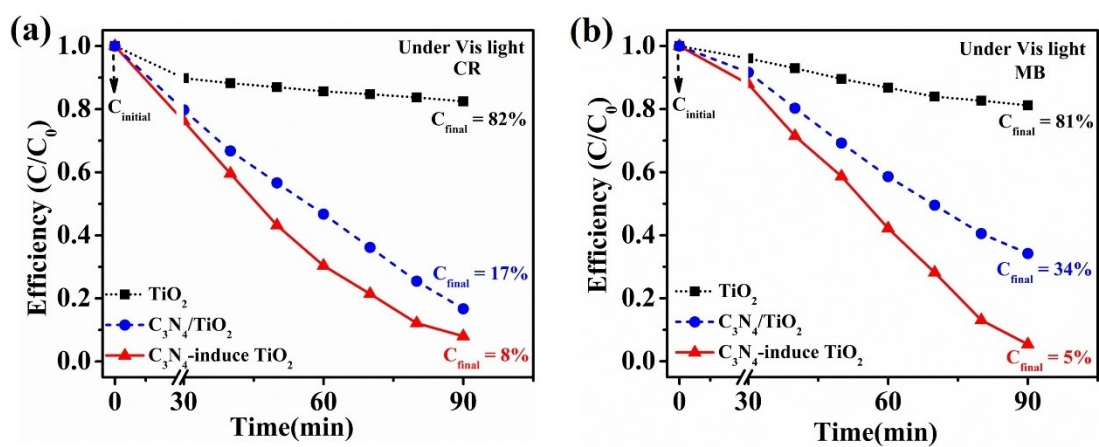
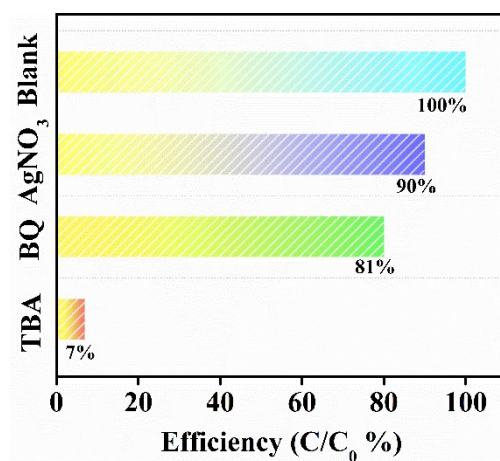


Figure S15. Standard curves of absorbance as a function of CR and MB concentration.





**Figure S16.** Photocatalytic degradation of (a) CR and (b) MB.



**Figure S17.** Photocatalytic degradation efficiency with the introduction of TBA ( $\cdot\text{OH}$ ),  $\text{AgNO}_3$  ( $e^-$ ) and BQ ( $\text{O}_2^-$ ) as scavengers during the degradation of Rh-b.

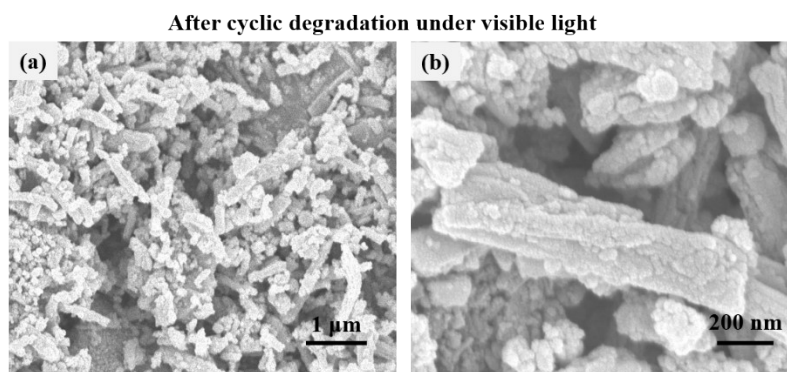


**Figure S18.** (a) SEM image and (b) magnified image of  $C_3N_4$ -induced  $TiO_2$  after cyclic degradation under visible light.

**Table S1.** Comparison of average crystallite size of  $TiO_2$  in  $C_3N_4$ -induced  $TiO_2$  as compared with other counterparts.

<b>Sample</b>	<b>Phase</b>	<b>Average crystallite size (nm)</b>
<b><math>TiO_2</math></b>	<b>Anatase</b>	<b>12.1</b>
<b><math>C_3N_4/TiO_2</math></b>	<b>Anatase</b>	<b>18.9</b>
<b><math>C_3N_4</math>-induced <math>TiO_2</math></b>	<b>Anatase</b>	<b>9.5</b>